

# Morphology of high-pressure crystallized poly(ethylene 2,6-naphthalate)

Liangbin Li<sup>a,b,\*</sup>, Chunmei Wang<sup>c</sup>, Rui Huang<sup>a</sup>, Ling Zhang<sup>a</sup>, Shiming Hong<sup>a</sup>

<sup>a</sup>Department of Polymer Materials Science and Engineering, Sichuan University, Chengdu 610065, People's Republic of China

<sup>b</sup>FOM-Institute of Atomic and Molecular Physics, Kruislaan 407, 1098 SJ Amsterdam, Netherlands

<sup>c</sup>Institute of Science, Nanjing University of Aeronautics and Astronautics, Nanjing 210016, People's Republic of China

Received 30 November 2000; received in revised form 6 February 2001; accepted 10 February 2001

## Abstract

The high-pressure crystallized poly(ethylene 2,6-naphthalate) (PEN) samples were investigated using wide-angle X-ray diffraction (WAXD), differential scanning calorimetry (DSC) and scanning electron microscopy (SEM). DSC results showed that the melting temperature of high-pressure crystallized PEN samples was up to 603 K, which is much higher than the equilibrium melting point of PEN suggested by Buchner et al. and near to the value estimated by Cheng et al. The striations in the morphology of PEN extended-chain crystals with thickness of about 1.5  $\mu\text{m}$  were observed with SEM. Some characteristic spherulitic forms obtained at high pressure are also presented. © 2001 Elsevier Science Ltd. All rights reserved.

**Keywords:** Poly(ethylene 2,6-naphthalate); High-pressure crystallization; Extended-chain crystals

## 1. Introduction

Poly(ethylene 2,6-naphthalate) (PEN) is a crystallizable polymer of increasing commercial interest that can be used in higher temperature applications than poly(ethylene terephthalate) (PET). The naphthalene ring provides greater rigidity to the polymer backbone than the benzene ring in PET, decreasing the crystallization rate.

Many studies on the crystallization behaviors of PEN have been reported. Buchner et al. [1] reported that PEN can crystallize into two different crystal modifications. The  $\alpha$  crystal form can be obtained by annealing amorphous PEN in the solid state, and the other crystal form ( $\beta$ ) can be obtained, but the  $\alpha$  form inevitably coexists when PEN is crystallized conventionally from the melt. During the past decade, PEN has been the subject of many morphological studies using X-ray diffraction (XRD) [2,3], differential scanning calorimetry (DSC) [4], infrared [5] and solid-state NMR spectroscopy [6], but not much work was carried out using scanning electron microscopy (SEM). On the other hand, many researchers have investigated the effects of external fields, such as solvent [7], shear [8], drawing [9] and flow [10] on the crystallization behaviors of PEN; no investigation was performed at high pressure.

In previous papers, we reported that PET extended-chain

crystals can be obtained through high-pressure crystallization and presented some novel spherulitic forms in high-pressure crystallized PET [11–13]. In this work, SEM and DSC were employed to investigate the morphology of high-pressure crystallized PEN samples. Samples with melting temperature up to 603 K were obtained and extended-chain crystals of PEN were observed. The rigidity brought out by naphthalene ring on the crystallization was also discussed.

## 2. Experimental

The PEN with an intrinsic viscosity of 0.65 dl/g used in this study was supplied in pellet form by ICI Co. Prior to the high-pressure treatment, the original PEN material was allowed to stand for 36 h at 368 K in vacuum to eliminate moisture. High-pressure experiments were carried out with a piston-cylinder high-pressure apparatus [14]. The following procedure for crystallization was used. After loading the sample, low pressure (20 MPa) was applied and temperature was raised to a predetermined level. After equilibrium was established, pressure was raised to the predetermined level. The samples were kept under these conditions for a predetermined time, and then quenched down to ambient condition. This procedure ensured that the polymer temperature would not exceed the crystallization temperature so as to minimize the degradation of PEN at elevated temperature and also to ensure that the polymer would be in

\* Corresponding author. Address: FOM-Institute of Atomic and Molecular Physics, Kruislaan 407, 1098 SJ Amsterdam, Netherlands.

E-mail address: liangbin@amolf.nl (L. Li).

Table 1  
The high-pressure crystallization conditions and results

Sample	Crystallization conditions	Melting temperature (K)	Melting enthalpy (J/g)	Crystallinity (%)
PEN1	300 MPa, 603 K, 6 h	552.31	64.59	62.5
PEN2	300 MPa, 623 K, 6 h	552.32	64.39	62.3
PEN3	300 MPa, 603 K, 24 h	554.03, 598.64	61.44, 21.69	80.1
PEN4	300 MPa, 603 K, 42 h	554.12, 600.71	58.76, 22.41	78.8
PEN5	300 MPa, 603 K, 48 h	554.27, 601.11	54.36, 21.56	73.4
PEN6	400 MPa, 603 K, 24 h	548.72, 602.94	60.67, 19.16	77.2
PEN7	400 MPa, 603 K, 30 h	552.24, 603.57	65.94, 23.31	86.3
PEN8	400 MPa, 603 K, 36 h	554.94, 603.55	66.38, 23.77	87.2

a molten state before crystallization takes place. The crystallization conditions are listed in Table 1.

Calorimetric measurements were performed at atmospheric pressure by using a Perkin–Elmer DSC-2 instrument. The calorimeter was calibrated with standard substance, which melts in the range of PEN. The heating rate was 10 K/min. The crystallinity was calculated with the following equation:

$$X_c = \Delta H_m / \Delta H_m^0 \quad (1)$$

where  $\Delta H_m^0$  is the equilibrium melting enthalpy, which was 103.4 J/g suggested by Cheng et al. [4].

SEM was carried out on an AMRAY1845FM apparatus, which was operated at 20 kV. Fracture of specimens was conducted at liquid N<sub>2</sub> temperature. Wide-angle X-ray diffraction (WAXD) was obtained at room temperature with a D/max-1-a instrument.

### 3. Results and discussion

#### 3.1. WAXD result

Fig. 1 gives out a representative WAXD profile of these high-pressure crystallized PEN samples. All main diffraction lines corresponded to the  $\beta$  crystal form, which can be crystallized from melt at normal pressure [1]. However, the intensity of (2 $\bar{4}$ 2) is too strong, compared with the report in Ref. [1]. Recently, Van den Heuvel and Klop [3] reported the different crystal constants for  $\beta$  modification in fiber. The peak (2 $\bar{4}$ 2) should be (200), and the intensity is in agreement with their report, but we cannot assign the peak ( $\bar{1}\bar{1}$ 1) in Fig. 1. This shows that  $\beta$  is sensitive to the experimental conditions. The small peak at the lower angle side foot of ( $\bar{1}\bar{1}$ 1) peak implied that the form possibly existed in these samples. Detailed investigation on the effect of high pressure on the crystal structures of PEN is being performed in our group.

#### 3.2. DSC measurements

Fig. 2 shows the DSC curves of these high-pressure crystallized PEN samples. The melting temperature ( $T_m$ ), melting enthalpy ( $H_m$ ) and crystallinity ( $X_c$ ) were also listed

in Table 1. PEN1 and 2 had a melting temperature of about 552.3 K, which is lower than the highest melting temperature (565 K) of PEN sample crystallized at atmospheric pressure [1]. This melting peak should correspond to folded-chain crystals of PEN. Although PEN2 was treated at temperatures higher than that of PEN1, the melting point and melting enthalpy had little difference. This seems to imply that the high-pressure crystallization behavior of PEN was possibly not affected significantly by temperature.

PEN3–5 were crystallized at same pressure and temperature but for 24, 42 and 48 h, respectively. They all had two melting temperatures. The low melting peak (about 554 K) in the DSC curve was near the melting temperature in PEN1 and 2, which also corresponded to folded-chain crystals of PEN. The other high melting temperature (about 600 K) was 35 K higher than the highest melting point of PEN sample crystallized at normal pressure, and even higher than the equilibrium melting temperature (573 K) of PEN suggested by Buchner et al. [1]. Cheng et al. [4] estimated that the equilibrium melting point of PEN was about 610 K. The

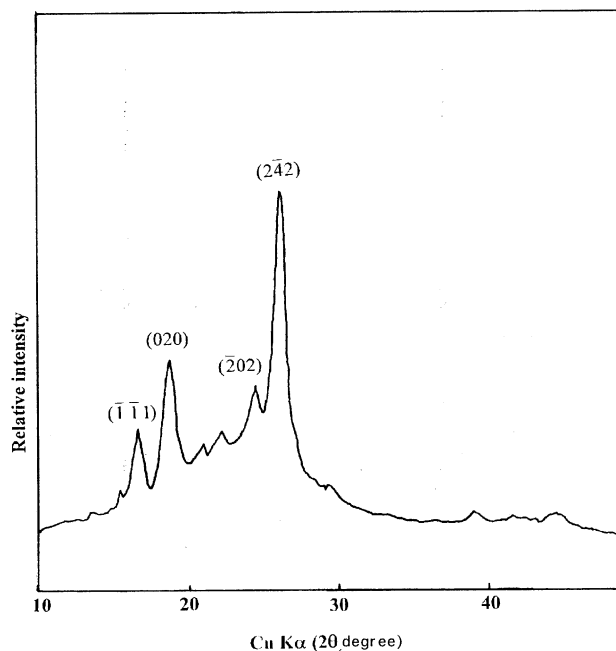


Fig. 1. WAXD profile of high-pressure crystallized PEN1.

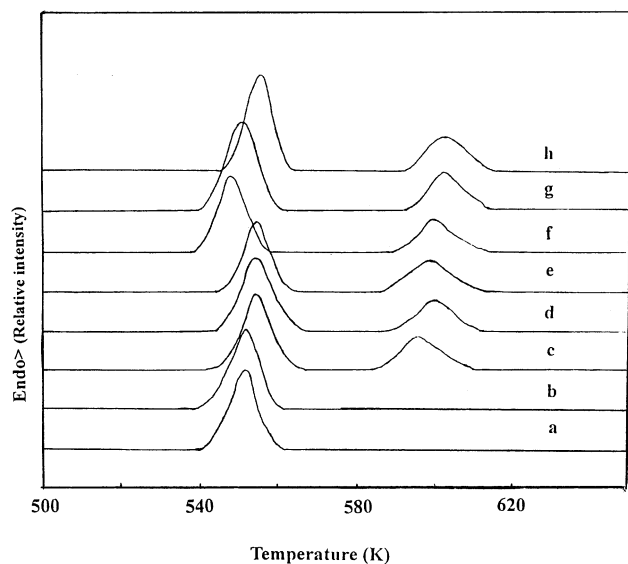


Fig. 2. DSC curves of PEN samples crystallized at (a) PEN1, 300 MPa, 603 K for 6 h; (b) PEN2, 300 MPa, 623 K for 6 h; (c) PEN3, 300 MPa, 603 K for 24 h; (d) PEN4, 300 MPa, 603 K for 24 h; (e) PEN5, 300 MPa, 603 K for 48 h; (f) PEN6, 400 MPa, 603 K for 24 h; (g) PEN7, 400 MPa, 603 K for 30 h; (h) PEN8, 400 MPa, 603 K for 36 h.

high melting temperatures of PEN3–5 were near to this value. Because WAXD already revealed that no new crystal form was crystallized at high pressure, the high melting temperatures should be assigned to extended-chain crystals of PEN. Along with the increase in crystallization time, the high melting temperature increased, and the low melting point changed slightly. The increase in the melting temperature may be due to the thickening growth of lamellar crystals. The decrease in melting enthalpy may be induced by degradation, which commonly occurs in polyester.

PEN6–8 were obtained at 400 MPa, 603 K for 24, 30 and 36 h, respectively. Two melting temperatures emerged in

the DSC measurement curves of every sample. The low (about 550 K) and high (603 K) melting temperatures may correspond to folded-chain and extended-chain crystals, respectively. This indicated that extended-chain crystals were possibly obtained in these PEN samples. The melting point and enthalpy increased with the increase in crystallization time under these conditions, which was different from that of PEN3–5. This was due to higher pressure and shorter crystallization time of PEN6–8. Higher pressure can inhibit high-temperature degradation in order to increase the melting enthalpy.

The above DSC results revealed that longer crystallization time is necessary to obtain PEN samples with high melting point. But longer crystallization time would increase the effect of degradation on PEN molecular chain. Balance crystallization conditions should be used to grow high melting point PEN samples, which is also the crucial problem to crystallize extended-chain crystals of rigid chain polymers.

### 3.3. SEM observations

All samples were detected with SEM. The fracture surfaces were not treated with any etching technique, but spherulitic forms of PEN were exposed clearly. The secondary electron images (SEI) of spherulites and an edge in PEN1 were shown in Figs. 3a and b, respectively. We could observe not only the characteristic round area but also some branches within the spherulite, especially on its edge. Such features are usually detected through etching techniques. This was possibly due to the high-temperature degradation, which eroded off the amorphous region in a similar mechanism with other etching techniques, and made the morphology of spherulites emerged. Amorphous region among spherulites was observed on the fracture surface of PEN1. This revealed that the growth of spherulites in some directions was not hindered by impingement.

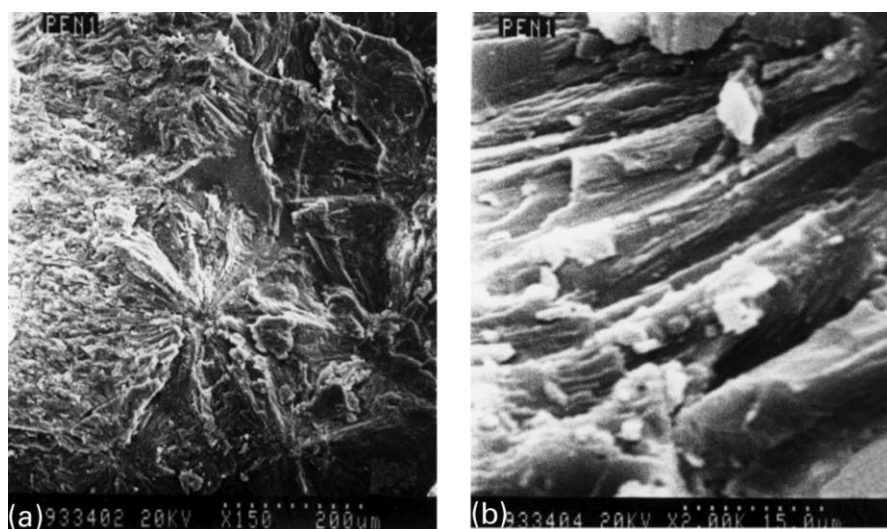


Fig. 3. Morphology of the spherulitic forms in PEN1 crystallized at 300 MPa, 603 K for 6 h.

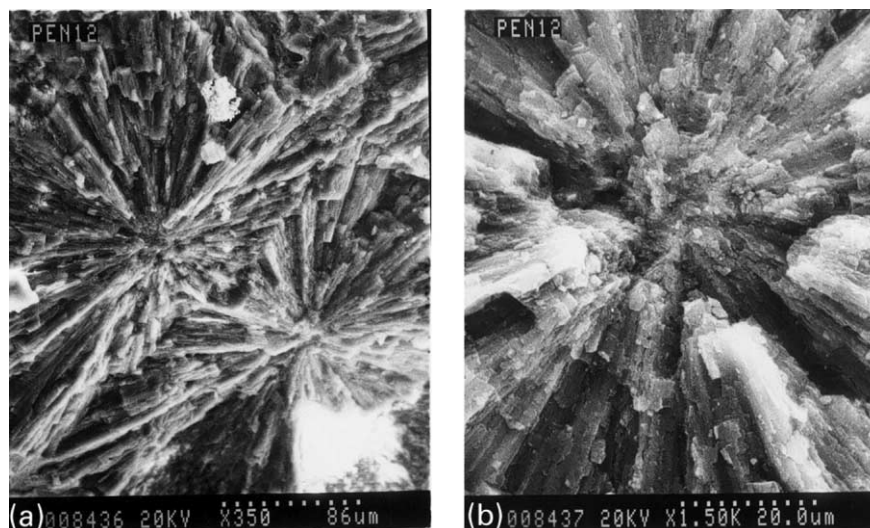


Fig. 4. Morphology of the spherulitic forms in PEN4 crystallized at 300 MPa, 603 K for 42 h.

The morphology of the fracture surface of PEN2 is similar to that of PEN1.

Fig. 4 displays two SEI of the fracture surface of PEN4. The branches within the spherulites were exposed clearer than those in PEN1. As PEN4 was crystallized for longer time, the spherulites grew mature and the effect of degradation on the amorphous region was more significant than that on PEN1. This made detailed structures within the spherulites expose more clearly.

A novel spherulitic form, which looked like a sunflower, was obtained in PEN7. Fig. 5a gives out a representative SEI of such spherulitic form. The sunflower-like spherulites were perhaps evolving through sheaf-like embryos before attaining a spherical envelope. The fracture surface may be the plane perpendicular to the sheaf and across the nucleus of the spherulite. Some interfaces of several spherulites

were shown in Fig. 5b. The spherulites impinged with one another and became polyhedral.

Spherulites were also observed in other samples. A common feature of these high-pressure crystallized PEN spherulites is that the growth along the radial direction was very straight as if it would not distort from the radial direction. This may reveal that the formation mechanism of these spherulites was different from that for PEN crystallized at much lower temperature and normal pressure [15]. Lee et al. [16] reported that the formation of polymer spherulites was connected with the denser structure in the induction period of polymer crystallization. We proposed that the growth could not be so straight along the radial direction as our high-pressure crystallized PEN spherulites if it adopted this mechanism.

The above DSC result indicated that extended-chain

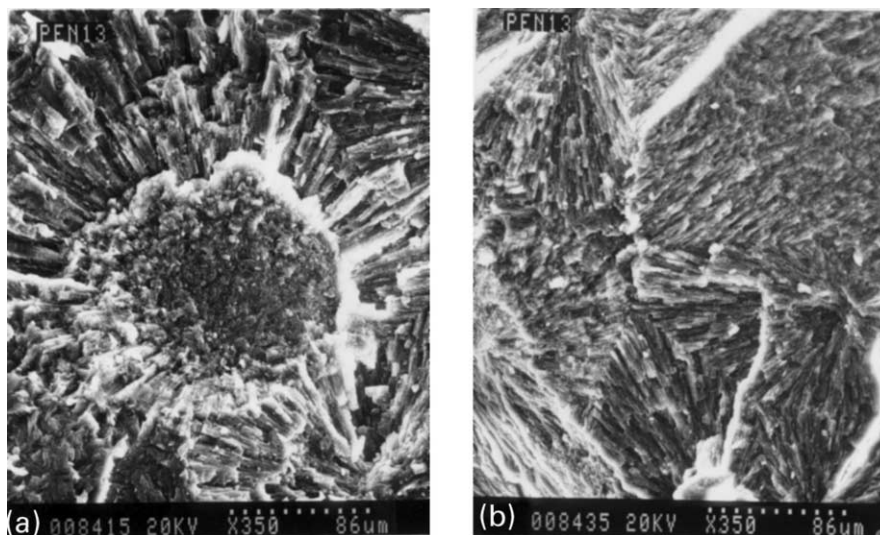


Fig. 5. Morphology of the spherulitic forms in PEN7 crystallized at 400 MPa, 603 K for 30 h.

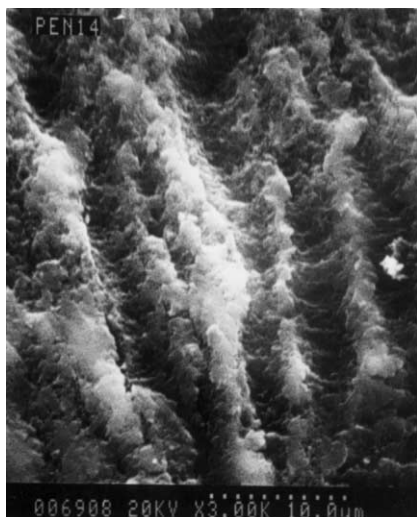


Fig. 6. Morphology of extended-chain crystals in PEN5 crystallized at 300 MPa, 603 K for 48 h.

crystals of PEN were possibly obtained in PEN4–8. Direct morphology should be given with SEM or TEM. Fig. 6 shows the SEI of the fracture surface of PEN5. The lamellar crystals in PEN5 were coarser than the extended-chain crystals of PET [11,12], but were similar to the extended-chain crystals of nylon6 [17]. This confirmed that the extended-chain crystals of PEN were obtained in PEN5. The coarse morphology of extended-chain crystals in PEN5 was due to the longer time degradation, which was also found in high-pressure crystallized PET samples [11].

The SEI of the fracture surfaces of PEN6 and 7 are shown in Figs. 7a and b, respectively. The parallel striations, which are the most common feature of polymer extended-chain crystals [18], could be clearly observed in Fig. 7. The thickness of extended-chain crystals in PEN6 and 7 is about 1.5  $\mu\text{m}$ , which is much longer than the length of molecular

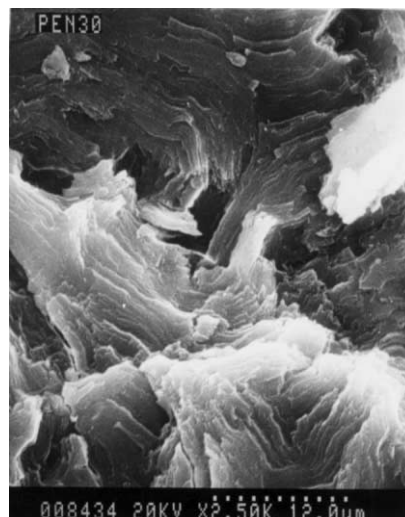


Fig. 8. Morphology of extended-chain crystals in PEN8 crystallized at 400 MPa, 603 K for 36 h.

chain. Extended-chain lamellar crystals with different features were also detected in PEN8. Fig. 8 displays the SEI of this kind of extended-chain crystals, which is similar to that of nylon11 [19].

Combining the DSC and SEM results, it is clear that extended-chain crystals of PEN can be obtained through high-pressure crystallization. However, longer crystallization time is necessary to grow PEN extended-chain crystals. The effect of high pressure on the extended-chain crystallization of PEN is more obvious than that of temperature. This is a little different from the results of high-pressure crystallized PET. It is not necessary to grow for longer time (more than 24 h) to crystallize extended-chain crystals of PET. This indicates that the rigidity of PEN molecular chain, increased by naphthalene ring, inhibits its diffusion rate and reduces the growth rate of crystals, especially the

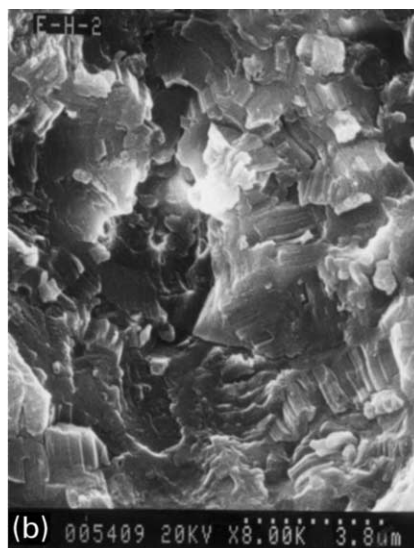
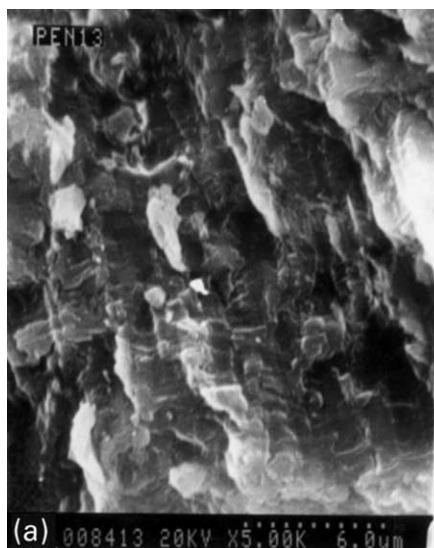


Fig. 7. Morphology of extended-chain crystals in (a) PEN6 and (b) 7 crystallized at 400 MPa, 603 K for 24 and 30 h, respectively.

thickening rate of lamellar crystals. So, compared with PET, extended-chain crystallization of PEN needs longer time. As degradation commonly occurs at high temperature in polyesters, more balance crystallization conditions would be introduced in for extended-chain crystallization of PEN at high pressure.

#### 4. Conclusion

Based on the WAXD, DSC and SEM results, it is concluded that extended-chain crystals of PEN can be obtained through high-pressure crystallization. Extended-chain crystals of PEN with a thickness of about 1.5  $\mu\text{m}$  were formed. The melting temperature of high-pressure crystallized PEN samples was up to 603 K, which is much higher than the equilibrium melting point of PEN suggested by Buchner et al. and near to the value estimated by Cheng et al. Some characteristic spherulitic forms obtained at high pressure were also presented.

#### Acknowledgements

The authors gratefully acknowledge the National Science Foundation as well as the Ministry of Education Foundation

for the financial support. The authors extend their gratitude to Professor Fu Qiang for helpful discussion.

#### References

- [1] Buchner S, Wiswer D, Zachmann HG. *Polymer* 1989;30:480.
- [2] Murakami S, Yamakawa M, Tsuji M, Kohjiya S. *Polymer* 1996;37:3945.
- [3] Van den Heuvel CJM, Klop EA. *Polymer* 2000;41:4249.
- [4] Cheng SZD, Wunderlich B. *Macromolecules* 1988;21:789.
- [5] Vasanthan N, Salem DR. *Macromolecules* 1999;32:6319.
- [6] Sata H, Kimura T, Ogawa S, Ito E. *Polymer* 1998;39:6325.
- [7] Kim SJ, Nam JY, Lee YM, Im SS. *Polymer* 1999;40:5623.
- [8] Yoon WJ, Myung HS, Kim BC, Im SS. *Polymer* 2000;41:4933.
- [9] Murakami S, Nishikawa Y, Tsuji M, Kawaguchi A, Kohjiya S, Cakmak M. *Polymer* 1995;36:291.
- [10] Okamoto M, Kubo H, Kotaka T. *Macromolecules* 1998;31:4223.
- [11] Li L, Huang R, Lu A, Nie F, Hong S, Wang C. *Polymer* 2000;41:6943.
- [12] Li L, Zhang L, Huang R, Fan W, Hong S. *J Polym Sci Phys Ed* 2000;38:1612.
- [13] Li L, Huang R, Lu A, Fan W, Hong S, Fu Q. *J Cryst Growth* 2000;216:538.
- [14] Fu Q, Huang R, Zhang X. *Sci China* 1994;A24:1218.
- [15] Balta Calleja FJ. *J Macromol Sci Phys* 1998;37:411.
- [16] Lee CH, Saito H, Inoue T. *Macromolecules* 1996;29:7034.
- [17] Gogolewski S, Pennings AJ. *Polymer* 1977;18:647.
- [18] Wunderlich B. *Macromolecular physics*, vol. 1. New York: Academic Press, 1973.
- [19] Gogolewski S, Pennings AJ. *Polymer* 1977;18:660.